24th COBEM - 2017

24th ABCM International Congress of Mechanical Engineering
December 3-8, 2017, Curitiba, PR, Brazil

COBEM-2017-0624
EXPERIMENTAL INVESTIGATIONS OF TURBULENCE PROMOTERS APPLIED TO HEAT TRANSFER APPLICATIONS

A.C. Campos
University of Campinas, School of Mechanical Engineering, Rua Mendeleyev, 200, Campinas, 13083-970, Brazil
alencardico@hotmail.com
T.S. Ferreira
Universidade de Brasília, Departamento de Engenharia Mecânica, Campus Darcy Ribeiro, Brasília, DF - Brazil
tatianasf.94@gmail.com
R.G. Gontijo
University of Campinas, School of Mechanical Engineering, Rua Mendeleyev, 200, Campinas, 13083-970, Brazil
rafaelgabler@fem.unicamp.br

Abstract.*The work provides an experimental investigation on the heat transfer rates exchanged between a heated device and a forced flow inside a channel. The focus of our approach is the evaluation of using turbulence promoters as a geometric alteration used to optimize the cooling process of electronic devices. The study is performed on a customized experimental bench, designed and built in the facilities of the Vortex Group at the University of Brasília. We present relevant results on the behaviour of the Nusselt number as a function of the Reynolds number for six different configurational arrangements of cylindrical-like turbulence promoters. We also present scaling laws that justify our findings. The influence of each geometry on the pressure drop inside the channel is also investigated for different Reynolds numbers.*

Keywords: *heat transfer, turbulence promoters, forced convection, electronic components, scaling laws*

1. INTRODUCTION

Whenever two bodies are subjected to a temperature difference, an energy interaction between them is established in the form of heat. The study of heat transfer processes is therefore fundamental in many areas of human knowledge, ranging from the study of large air and water masses movement processes (not only in the Earth's atmosphere, but also in our oceans) and in other planets heat transfer also occurs by convection that is associated with instability at the bottom of lithosphere plates Solomatov and Moresi (2000). until the development of new techniques in modern electronic devices cooling.

The heat transfer enhancement is a problem that has been broadly studied for a long time due to its importance in the development of new technologies. Nowadays, the market trend is reducing the area of the already-small electronic components, in order to make new devices, with greater capabilities and more functionality. With this miniaturization tendency of electronic components, heat dissipation becomes a problem, since the superficial area is one key factor to heat dissipation. That way, it is necessary to find ways to enhance the convective heat transfer in reduced areas. Most of the electronic devices rely on the convective heat transfer to cool down the components and there are many strategies to enhance that without increasing the area. It is possible to change the fluid used in the flow, for example with the addition of nanoparticles, as studied by Mohamad (2015a).You can also vary the angle of attack of the component, like Heidarzadeh *et al.* (2014a). Another possibility is the increase of the turbulence level. It can be done with the help of turbulence promoters, as done by Thomas (1967a), or with a ribbed channel, as done by Eiamsa ard and Changcharoen (2011a).

The application of rotational flows Huang and El-Genk (1998), introduction of vortex generators (Ianiro and Cardone, 2012; Violato *et al.*, 2012), perforated plates (Lee *et al.*, 2002) or meshes (Zhou and Lee, 2004; Zhou *et al.*, 2006) or even models of turbulent flows through numerical simulations (Gontijo and Rodrigues, 2011) are some of the proposals that have been studied. In these cases, the increase of heat exchange rates is obtained by the excitation / transformation of the organization of the turbulent structures present in the flow. This is the main physical mechanism responsible for maximizing heat transfer rates. The efficient use of the dissipation property in turbulent flows is the key to meaningfully optimize heat transfer processes involving fluid / structure interaction.

Knowing that different mechanisms may interfere in the process of heat transfer, the present work was developed with the purpose of investigating experimentally the increase of the heat transfer rates in an electronic component by forced convection using turbulence promoters. For this purpose, the variables that participate in the cooling process of

an electronic component such as the numbers Reynolds, Nusselt, Prandt, heat transfer coefficient, pressure drop and performance coefficiente were evaluated. A new database regarding the connection between the explored geometries and their effectiveness is presented.

2. EXPERIMENTAL PROCEDURE

The proposed experiment consists in verifying the Nusselt number in a small heated surface cooled by a flow in five different velocities and disturbed by six different turbulence promoters configurations. The turbulence promoters are cylinder arrangements and each configuration contains a different number of cylinders located in different positions, as it appears in Figure 1a. In order to verify wether the boundary condition on the surface of the Peltier cell is more closely to constant temperature or constant heat flux, we measured the time dependence of the surface temperature in the cell in 16 points in the absecence of the flow (figure 1b). It is possible to observe temperature differences of up to 10^oC through its surface (figure 1d). This non-uniform distribution is also observed in the thermal image shown in figure 1c. For this purpose we have considered that the thermal boundary condition on the surface of the cell is more close to a constant heat flux condition in our interpretation of the results, which may be seen as a simplification of the reality explored here.

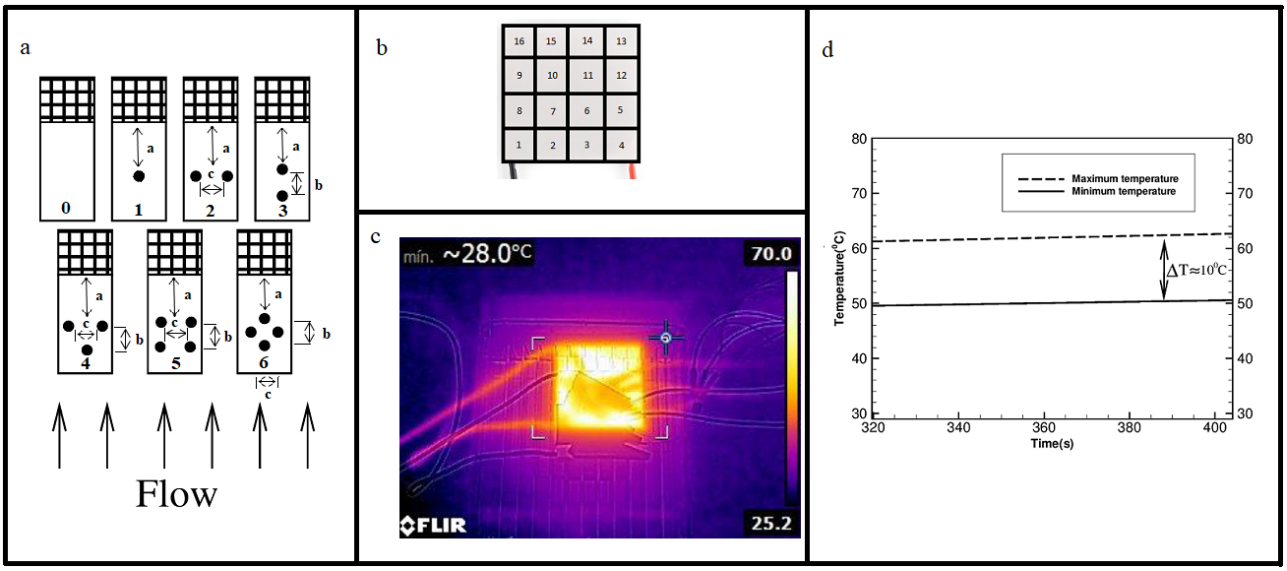

Figure 1. a)Models of the promoters used, where the hatch part represents the electronic component (superior view) and the respective distances between the promoters and the device and between the promoters themselves (a = 14 mm, b = 8 mm, c = 8 mm); b) Points on the surface of the Peltier cell considered for the evaluation of the temperature distribution on its surface; c)A typical view of the temperature field on the surface of the Peltier cell before turning on the wind tunnel. This image was obtained with a Flir E5 thermal camera; d)Temperature of the coolest (solid line) and hottest (dashed line) points in the cell as a function of time. These temperatures were measured with a LM-35 temperature sensor connected with an Arduino microprocessor.

The test bench used to the testing procedures was set at one of the Vortex Research Group's wind tunnels. The bench was stablished with an infrared MLX90614 temperature sensor, a Peltier cell as heat source and an Arduino microprocessor, connected to a computer to data acquisition, and a digital voltage regulator of type MPL-3303. A CR2032 digital anemometer was also used to measure the flow's velocity and outlet temperature. The bench, along with its components, is shown in Figure (2).

The wind tunnel was set to operate in five different flow velocities, chosen according to the wind tunnel engine power: 3 m/s, 6 m/s, 9 m/s, 12 m/s and 15 m/s. In order to obtain a graph comparing the Nusselt Number versus the Reynolds Number, it is known that:

$$Nu = \frac{hD}{k}, \tag{1}$$

$$Re = \frac{\rho v D}{\mu}, \tag{2}$$

where h is the convective heat transfer coefficient, D is the hydraulic diameter od the channel, k is the thermal conductivity for the air, ρ is the air's density, v the flow velocity and μ is dynamic viscosity of air. All thermophysical properties were evaluated at film temperature.

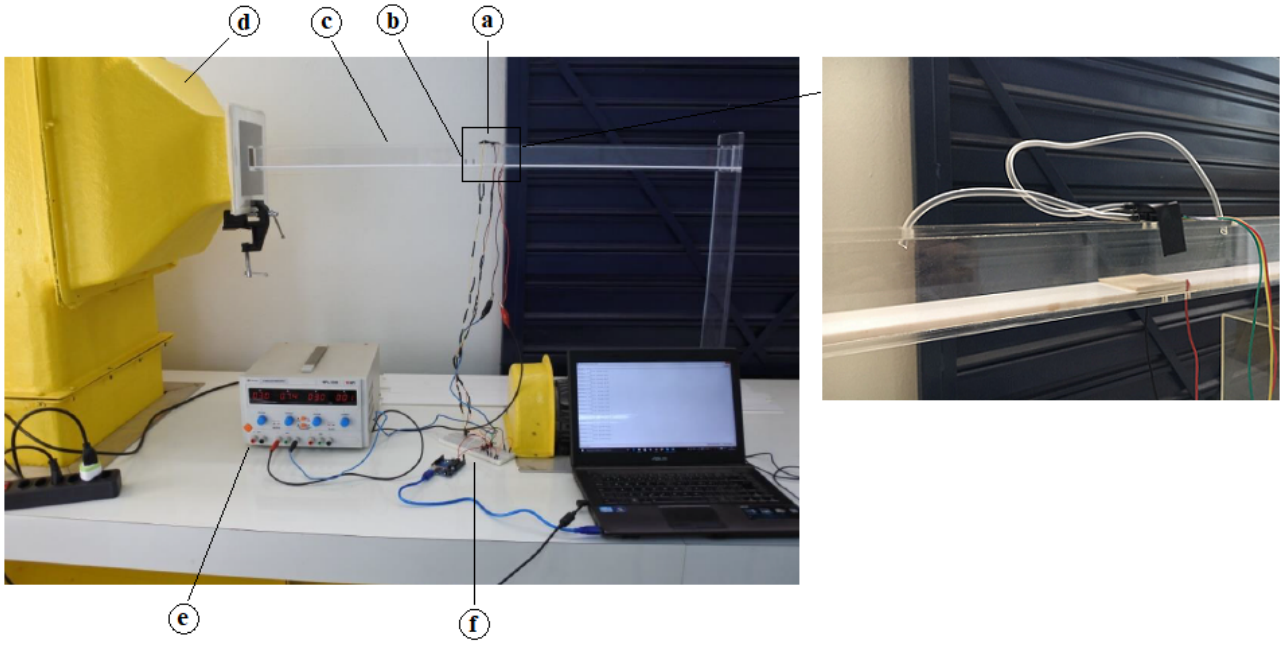

Figure 2. Experimental bench with the figure of the pressure sensor a)Infrared temperature sensor; b)Peltier cell and Cell's support with turbulence promoters attached; c)Test section; d)Wind tunnel; e)Tension source; f)Protoboard and Arduino conections;

It is also known that the heat flux can be expressed as a product between the convective heat transfer coefficient and the temperature difference. This flux, through dimensional analysis, has the unit of a power rating per area unit, making it possible the rewrite the heat flux as a ratio between the electric power and the superficial area of the Peltier cell. The electric power can be obtained from the product between the difference of electric potential and the current, both being measured through the digital voltage regulator. Here we assume that the Peltier cell works as a pure resistive electric circuit component. With that in mind, and using Newton's cooling law, the convective heat transfer coefficient becomes:

$$h = \frac{Ui}{A\Delta T}, \tag{3}$$

replacing eq. (3) in eq. (1), wet get:

$$Nu = \frac{UiD}{A\Delta Tk}, \tag{4}$$

where the ΔT is the difference between the Peltier cell's superficial temperature and the flow's outlet temperature.

In each velocity, for each one of the six different turbulence promoters configurations and for the free flow, five tests were made, making it possible to perform a statistical analysis of the experimental results. The average Nusselt number was calculated for each Reynolds number and the Nusselt number standard deviation was used as the error bar, according to equations (5) and (6) show.

$$\overline{Nu} = \frac{\sum_{i=1,}^{n} Nu_i}{n}, \tag{5}$$

$$\sigma_{Nu} = \sqrt{\sum_{i=1,}^{n} \frac{(Nu_i - \overline{Nu})^2}{i}}, \tag{6}$$

n = 5 and i = 5, since both represent the number of test achievements for each speed.

For the calculation of the pressure drop considering the uniform flow and a constant speed, the principle of Bernoulli, between two points can be written as follows:

$$\frac{P_1 - P_2}{\rho} = \frac{v_1 - v_2}{2} + g(y_2 - y_1) + P_c, \tag{7}$$

where y_1 and y_2 are the geometric heights in the direction of gravity at the two points, already P_1 (upstream) and P_2 (downstream) are the pressures and P_c represents the pressure drop. The points analyzed are at the same height, so

equation (7) can be rewritten as:

$$P_c = \frac{P_1 - P_2}{\rho}. \tag{8}$$

The mean pressures upstream and downstream of the Peltier cell were calculated as:

$$P_{mont} = \frac{\sum_{i=1}^{n} P_i}{n}, \tag{9}$$

$$P_{jus} = \frac{\sum_{i=1}^{n} P_i}{n}, \tag{10}$$

where P_{mont} represents the mean pressure measured before the turbulence promoters and P_{jus} is the mean pressure obtained after the turbulence promoters. The pressure sensors were placed at an horizontal distance of 12.5 cm before and 5.5 cm after the turbulence promoters. With these mean pressures, it was possible to calculate the average pressure drop for each of the five tests.

$$\Delta P_i = P_{mont} - P_{jus}. \tag{11}$$

With the values of the average pressure drop it was also possible to calculate the pressure coefficient. The mean pressure coefficient Cp_i for each velocity and turbulence promoter, their mean values $\overline{Cp}$ and the standard deviation σ_{Cp}.

$$Cp_i = \frac{\Delta P_i}{\rho u_i^2}, \tag{12}$$

$$\overline{Cp} = \frac{\sum_{i=1}^{n} Cp_i}{j}, \tag{13}$$

$$\sigma_{Cp} = \sqrt{\sum_{i=1,}^{n} \frac{(Cp_i - \overline{Cp})^2}{i}}. \tag{14}$$

With all these values found, it was possible to find the thermal performance for each support at each speed through the equation below:

$$\beta = \frac{Nu}{\overline{Cp}}. \tag{15}$$

The support without turbulence promoters is the control support β_0, so it was possible to compare the values of the other supports at all speeds with the control support through the ratio of the ratio $\frac{\beta}{\beta_0}$.

3. SCALING ARGUMENTS

It is known that turbulence can improve heat transfer rates due to its tridimensional mixing properties. The flow mixing and the secondary flows are responsible for the turbulence's heat transport Schlichting *et al.* (1955). In order to try to understand the physical mechanisms that promote the heat transfer enhancement in the turbulent flow, the starting point is the Energy equation.

$$\rho Cp \left[\frac{\partial T}{\partial t} + u\frac{\partial T}{\partial x} + v\frac{\partial T}{\partial y} + w\frac{\partial T}{\partial z}\right] = k\left[\frac{\partial^2 T}{\partial x^2} + \frac{\partial^2 T}{\partial y^2} + \frac{\partial^2 T}{\partial z^2}\right] + \Phi, \tag{16}$$

where ρ is the fluid's density,Cp is the especific heat at constant pressure, t is the time , T is the Eulerian temperature field, u, v and w are the respective velocity components in the x, y and z directions and k is the fluid's thermal conductivity.

In this case, the production of internal energy due to viscous dissipation mechanisms won't be considered due to the low viscosity of the air and to the small velocity gradients obtained in the experiment. To get to the turbulent mean temperature field the Reynold's average process is applied in the Energy Equation. The relations are shown in equation (17).

$$\begin{aligned} u &= \overline{u} + u' \\ v &= \overline{v} + v' \\ w &= \overline{w} + w' \\ T &= \overline{T} + T' \end{aligned} \tag{17}$$

This method shows one variable with two different parts: the average value and its turbulent flutuations. The average value is calculate through equation (18)

$$\overline{u} = \frac{1}{\tau}\int_0^\tau u\,\mathrm{d}t, \tag{18}$$

where τ is a long enough time for which the ergodicity hypothesis can be considered.

The turbulent flow can be considered statistically stationary, which allows the statistical properties to be applied to the Energy equation, then after some algebraic manipulation:

$$\overline{u}\frac{\partial\overline{T}}{\partial x} + \overline{v}\frac{\partial\overline{T}}{\partial y} + \overline{w}\frac{\partial\overline{T}}{\partial z} = \frac{1}{\rho C_p}\frac{\partial}{\partial y}\left[k\left(\frac{\partial\overline{T}}{\partial x} + \frac{\partial\overline{T}}{\partial y} + \frac{\partial\overline{T}}{\partial z}\right) - \rho C_p(\overline{u'T'} + \overline{v'T'} + \overline{w'T'})\right]. \tag{19}$$

It is known that the real flow is tridimensional, but the boundary layer approximation is enough for scaling analysis purposes, which leads to:

$$\overline{u}\frac{\partial\overline{T}}{\partial x} + \overline{v}\frac{\partial\overline{T}}{\partial y} = \frac{1}{\rho C_p}\frac{\partial}{\partial y}\left(k\frac{\partial\overline{T}}{\partial y} - \rho C_p\overline{v'T'}\right). \tag{20}$$

The last term of equation (20) is a heat flux, since it adds to the Fourier's Law, which is:

$$q'' = -k\frac{\partial T}{\partial y} = -\rho C_p\alpha\frac{\partial T}{\partial y}, \tag{21}$$

where α is the thermal difusivity.

Also, the last term of equation (29) is related to turbulent fluctuations and represents an additional unknown variable. The modeling of this term can be made through an analogy with Boussinesq's Hypothesis. Through Newton's viscosity Law, a turbulent viscosity is found. The same steps will be taken to find a turbulent themal difusivity through Fourier's heat conduction Law. It is shown in equations (22) and (23).

$$-\rho\overline{u'v'} = \mu_T\frac{\partial\overline{u}}{y}, \tag{22}$$

$$-\rho C_p\overline{v'T'} = \rho C_p\alpha_T\frac{\partial\overline{T}}{\partial y}, \tag{23}$$

where μ_T is the turbulent viscosity and α_T is the turbulent thermal difusivity. Replacing Equation (23) in Equation (20):

$$\overline{u}\frac{\partial\overline{T}}{\partial x} + \overline{v}\frac{\partial\overline{T}}{\partial y} = \frac{\partial}{\partial y}\left(\alpha + \alpha_T\frac{\partial\overline{T}}{\partial y}\right). \tag{24}$$

Shifting the analysis to the Nusselt number, it can be split in two parts: a laminar and a turbulent contribution, as shown in equations (25) to (27).

$$Nu = Nu_L + Nu_T, \tag{25}$$

$$Nu_L = \frac{h_L L}{k}, \tag{26}$$

$$Nu_T = \frac{h_T L}{k}, \tag{27}$$

where L is the characteristic dimension of the flow channel and h_L and h_T are, respectively, the convective heat transfer coefficients for laminar and turbulent flow. Those coefficients can be rewritten as:

$$h_L = \frac{q''_L}{\Delta T}, \tag{28}$$

$$h_T = \frac{q''_T}{\Delta T}, \tag{29}$$

where ΔT is the difference between the plate's superficial temperature and the flow's temperature. From Equations (28) and (29):

$$q''_L = \alpha\rho C_p\frac{\partial\overline{T}}{\partial y}, \tag{30}$$

$$q''_T = \alpha_T \rho C_p \frac{\partial \overline{T}}{\partial y}. \tag{31}$$

After some algebraic manipulation between Equations (26) to (31), the result is:

$$Nu_L = \frac{\alpha \rho C_p}{\Delta T} \frac{\partial \overline{T}}{\partial y} \frac{L}{k}, \tag{32}$$

$$Nu_T = \frac{\alpha_T \rho C_p}{\Delta T} \frac{\partial \overline{T}}{\partial y} \frac{L}{k}. \tag{33}$$

In order to find the Nusselt number scale, the scale of its paramethers must be defined. The scale of $\partial\, \bar{T}$ is $\bar{T}$ and, for the y axis, the thermal boundary layer thickness, δ_T, is the used scale for the laminar share, and the lenght *l*, the typical scale to which the vortex dissipate heat, is the scale for the turbulent share, then:

$$Nu_L \sim \frac{\alpha \rho C_p L}{\delta_T k}, \tag{34}$$

$$Nu_T \sim \frac{\alpha_T \rho C_p L}{kl}. \tag{35}$$

From Equation (25):

$$Nu \sim \frac{L}{\delta_T} + \frac{\alpha_T}{\alpha} \frac{L}{l}. \tag{36}$$

To fulfill the analysis, the modeling of α_T must be done. It will be done through the definition of turbulent Prandtl number from Jones and Launder (1972):

$$Pr_T = \frac{\upsilon_T}{\alpha_T}, \tag{37}$$

where υ_T is the turbulent viscosity, yet to be modeled. Replacing equation (37) in equation (36):

$$Nu \sim \frac{L}{\delta_T} + \frac{\upsilon_T}{Pr_T \alpha} \frac{L}{l}. \tag{38}$$

Taking $Pr \simeq 1$, from the classical scaling analysis:

$$\frac{\delta_t}{L} \sim Re^{\frac{1}{2}}, \tag{39}$$

here we use the classical scaling for a laminar boundary flayer flow over a flat plate. This point will be justified later due to the very low values of pressure drop found though the experiments. Where *Re* is the Reynolds number. Replacing equation (39) in equation (38):

$$Nu \sim Re^{\frac{1}{2}} + \frac{\upsilon_T}{Pr_T \alpha} \frac{L}{l}. \tag{40}$$

The modeling of υ_T will be done through the *k* - ϵ model:

$$\upsilon_T = \frac{C_\mu k^2}{\varepsilon}, \tag{41}$$

where C_μ is the model's calibration constant, ε is turbulent kinetic energy dissipation and *k* is the turbulent kinetic energy, calculated through equation (42):

$$k = \frac{\overline{u'^2 + v'^2 + w'^2}}{2}. \tag{42}$$

From Jones and Launder, the scale analysis for the turbulent kinetic energy dissipation is:

$$\varepsilon \sim \frac{k^{\frac{3}{2}}}{l}. \tag{43}$$

Working with equations (43), (41) and (40), the result is:

$$Nu \sim Re^{\frac{1}{2}} + \frac{C_\mu k^2}{k^{\frac{3}{2}} Pr_T \alpha} L. \tag{44}$$

As C_μ and Pr_T are known numbers, the final result for the scale analysis is:

$$Nu \sim Re^{\frac{1}{2}} + \frac{k^{\frac{1}{2}} L}{\alpha}. \tag{45}$$

This result shows that the Nusselt number rises with the square root of the turbulent kinetic energy, which means the heat transfer can rise with turbulence increase. Considering a typical scale for the turbulent kinetic energy $\kappa \sim v^2 Re^{-1/2}$ we get:

$$Nu \sim Re^{1/2} \left(1 + Re^{3/2}\right). \tag{46}$$

The main purpose of this scale analysis is to prove why it is possible, mathematically, to increase the heat transfer by adding turbulence promoters to a channel. However, it is known that the turbulence is a tridimensional non-linear phenomenon, that is why experimental results are also needed.

4. RESULTS

Following the experimental procedure and according to the proposed scaling it was possible to plot the graphs (3) and (4) of the Nusselt number in function of the Reynolds number. The graphs represent the behavior of the cooling process in the Peltier cell.

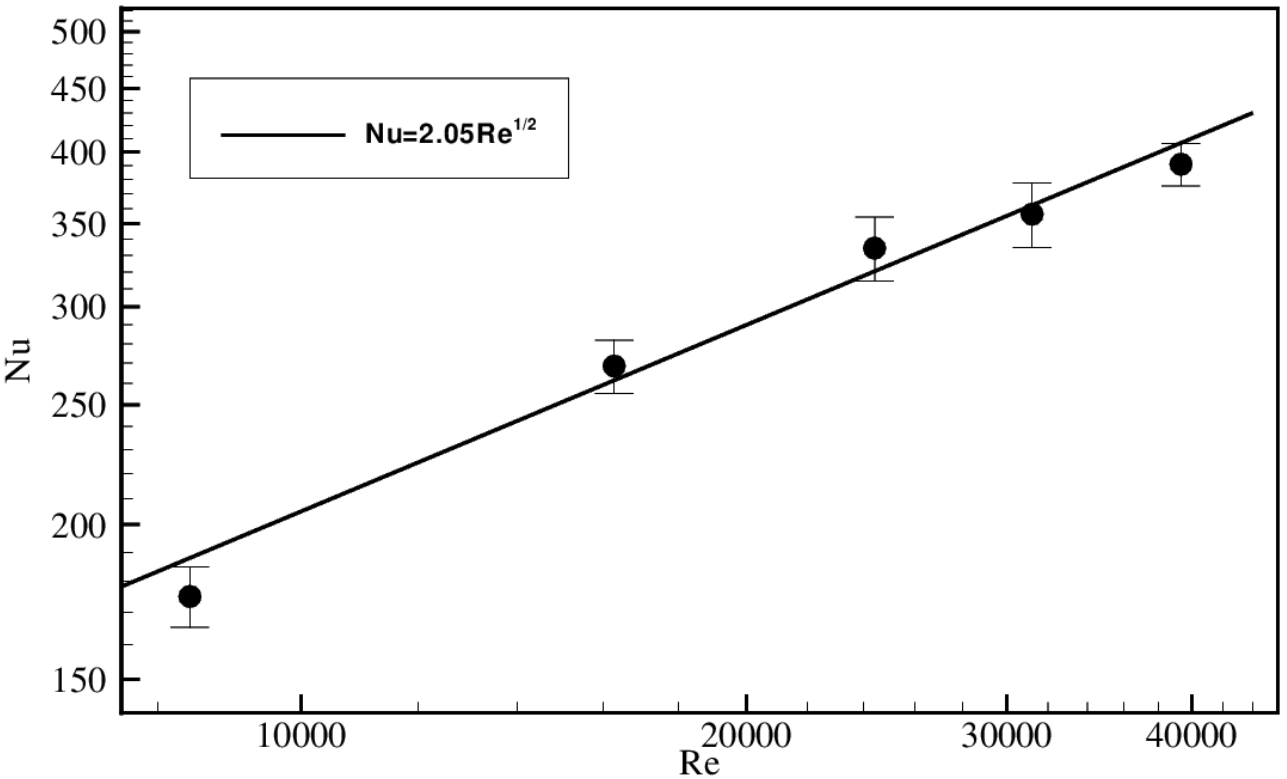

Figure 3. Graph of the Nusselt number as a function of the Reynolds number of support 1 with turbulence promoter with the scaling of Nu=Re$^{1/2}$.

Figure (3) shows the behavior of the global Nusselt number as a function of the Reynolds number of the flow, based on the hydraulic diameter. This curve was made for the turbulence promoter number 1. A good agreement is observed between the experimental behavior and the classic scaling for laminar regime, in which $Nu \sim Re^{\frac{1}{2}}$. This result is an indicative that the geometry of the promoter used is not capable of generating turbulent structures that substantially modify the expected behavior for the case without a turbulence promoter, They also indicate a possible laminarization of the flow through the use of support number 1.

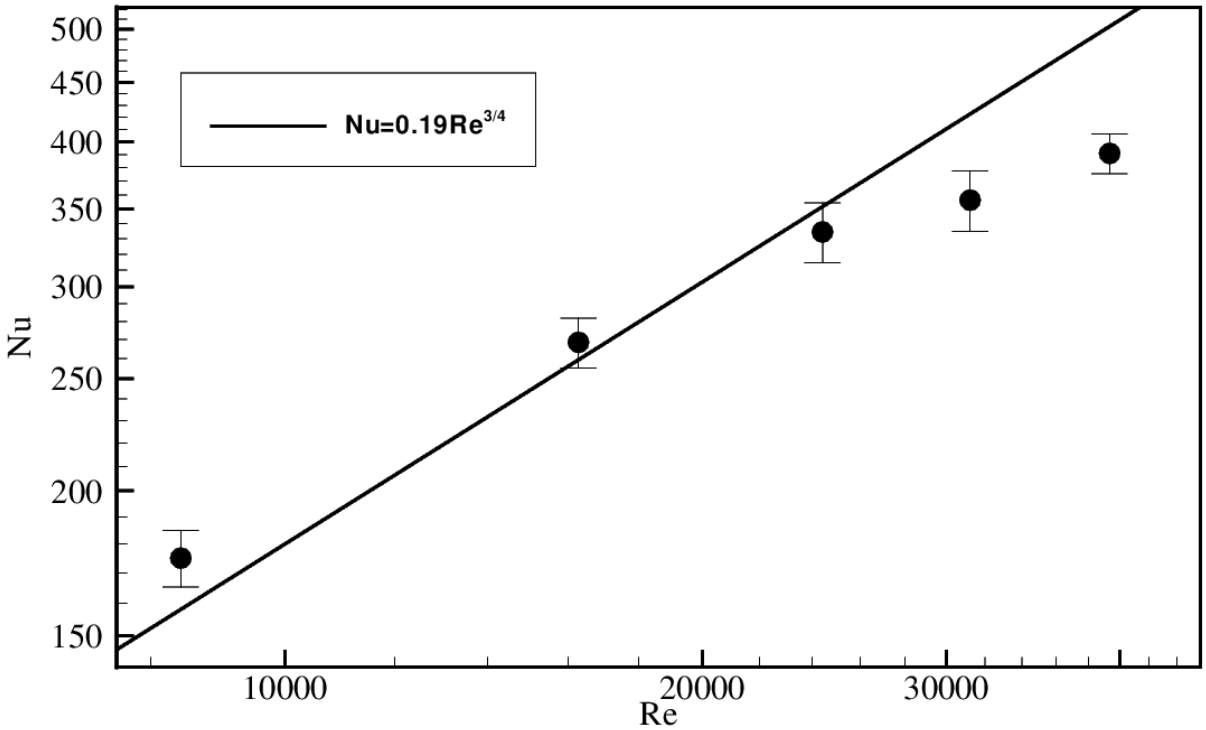

Figure 4. Graph of the Nusselt number as a function of the Reynolds number of support 2 with turbulence promoter with the scaling of Nu=Re$^{3/4}$.

Figure (4) shows the behavior Nu x Re for the turbulence promoter number 2. For this case it is possible to observe that in the range $8140 \leq Re \leq 24420$, the nature of the turbulent structures formed therein is compatible with the scaling proposed in the present work. However, it is noted that for $Re > 24420$ the same scaling is not able to predict the experimental functional relationship $Nu = f(Re)$ properly. Indicating that for this specific promoter geometry there is not an universal scaling of the power law type valid for all Reynolds number ranges.

By calculating the pressure drop it was also possible to calculate the thermal performance. Figure (5) compares the values found for support 2 without turbulence promoters.

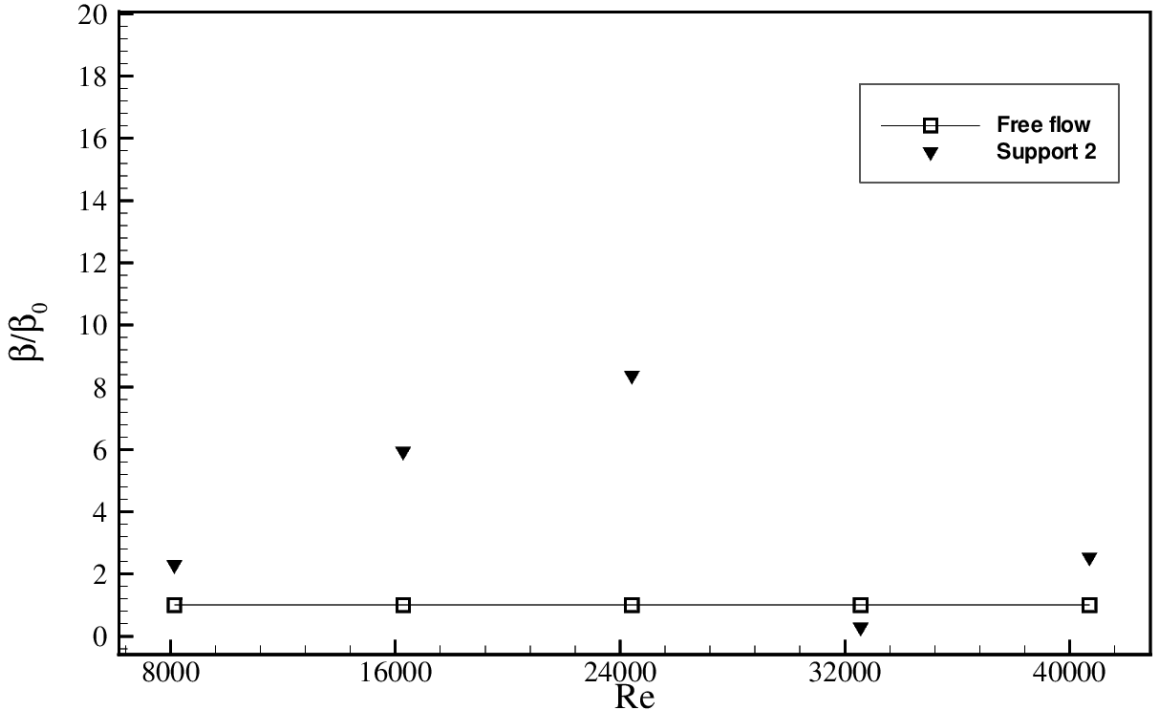

Figure 5. Thermal performance chart

As expected, support 2 was the one that obtained the best performance. This is due to support 2 having higher Nusselt numbers and lower pressure drop values. It is also important to highlight that it seems to be an optimal Reynolds ($Re_D = 24200$) for which the performance is approximately 10 times greater than the control case (without turbulence promoters).

It was possible, through the results found, to realize that in average terms the turbulence promoters increased the rate of heat transfer, compared to the support that did not contain turbulence promoters. It was possible to notice that support number 2 was the best configuration tested, since it presented higher cooling rates elevations at all speeds. The following table presents the values found for support 2.

Table 1. Results for turbulence promoter support 2

Velocity (m/s)	3	6	9	12	15
Reynolds number	8140	16280	24420	32561	40701
Voltage (V)	3.1	2.9	2.9	2.8	2.8
Current (A)	0.74	0.74	0.74	0.74	0.74
ΔT Teste 1 ($^\circ$C)	11.50	7.46	5.78	5,26	5,29
ΔT Teste 2 ($^\circ$C)	11.27	7.32	5.92	5.21	5.05
ΔT Teste 3 ($^\circ$C)	11.52	7.21	5.90	5.59	5.11
ΔT Teste 4 ($^\circ$C)	10.99	7.30	6.18	5.61	5.47
ΔT Teste 5 ($^\circ$C)	11.09	7.21	5.83	5.32	5.22
Nu medium	202	293	361	382	395
Standard deviation Nu	3.8367	3.6381	8.1962	11.7541	10.8303
ΔP medium (kPa)	0.0019761	0.0006825	0.00063492	0.0066322	0.00046031
Standard deviation	0.00331156	0.00141514	0.00085405	0.00746141	0.00241517
Performance (β/β_0)	2.294	5.939	8.380	0.283	2.536

Still on the second support in the last two Reynolds values, the Nusselt numbers were slightly altered when compared to the increases that occurred in the first three Reynolds values. It can also be noticed that at speed 9 m/s all the rulers with turbulence promoters had higher Nusselt numbers. The results obtained for the velocity of 9 m/s are interesting because this velocity represents average operational values of interest in conventional processing chillers used in microprocessors. The performance values of each support for the five Reynolds numbers in relation to the control support (without turbulence promoters) are presented in the following table.

Table 2. Relative performance relative to control support (β/β_0)

Reynolds number	8140	16280	24420	32561	40701
Support number 1	0.787	0.872	1.945	0.538	0.237
Support number 2	2.294	5.939	8.380	0.283	2.536
Support number 3	1.149	0.694	0.883	0.695	0.334
Support number 4	1.503	1.028	1.094	0.383	1.882
Support number 5	18.128	2.035	3.678	0.757	0.357
Support number 6	0.345	0.242	0.395	0.140	0.066

5. CONCLUDING REMARKS

From all the measurements we found that the supports using turbulence promoters presented an increase on the heat transfer rates, except for support 6 at speeds of 12 and 15 m/s. We argue that this decrease when compared to the control case (no turbulence promoter) has occurred due to the formation of low pressure zones on the heated surface which acted as heat dissipation blockers. Regarding the overall performance, we have noted that despite the increase in the heat transfer rates, several combinations of geometry and Reynolds number have provided a pressure drop increase which ended up with a net performance bellow the control case. The configuration which presented the best performance for the highest Reynolds range was the use of two side-by-side cylinders before the leading edge of the heated device.

6. ACKNOWLEDGEMENTS

The authors wish to acknowledge the following institutions and grants for the support of this work: CNPq-Brazil under the Grant Nº, 441496/2014-8 and FAPDF-Brazil under the Grants Nº 4322.25.2991326062015.

7. REFERENCES

Eiamsa ard, S. and Changcharoen, W., 2011a. "Analysis of turbulent heat transfer and fluid flow in channels with various ribbed internal surfaces". *Journal of Thermal Science*, Vol. 20, pp. 260–267.

Gontijo, R.G. and Rodrigues, J.L.A.d.F., 2011. "The numerical modeling of thermal turbulent wall flows with the classical κ-ε model". *Journal of the Brazilian Society of Mechanical Sciences and Engineering*, Vol. 33, No. 1, pp. 107–116.

Heidarzadeh, H., Farhadi, M. and Sedighi, K., 2014a. "Convective heat transfer over a wall mounted cube at different angle of attack using large eddy simulation". *Thermal Science*, Vol. 18, pp. 301–315.

Huang, L. and El-Genk, M., 1998. "Heat transfer and flow visualization experiments of swirling, multi-channel, and conventional impinging jets". *International Journal of Heat and Mass Transfer*, Vol. 41, No. 3, pp. 583–600.

Ianiro, A. and Cardone, G., 2012. "Heat transfer rate and uniformity in multichannel swirling impinging jets". *Applied Thermal Engineering*, Vol. 49, pp. 89–98.

Jones, W. and Launder, B., 1972. "The prediction of laminarization with a two-equation model of turbulence". *International journal of heat and mass transfer*, Vol. 15, No. 2, pp. 301–314.

Lee, D.H., Lee, Y.M., Kim, Y.T., Won, S.Y. and Chung, Y.S., 2002. "Heat transfer enhancement by the perforated plate installed between an impinging jet and the target plate". *International journal of heat and mass transfer*, Vol. 45, No. 1, pp. 213–217.

Mohamad, A., 2015a. "Myth about nano-fluid heat transfer enhancement". *International Journal of Heat and Mass Transfer*, Vol. 86, pp. 397–403.

Schlichting, H., Gersten, K., Krause, E. and Oertel, H., 1955. *Boundary-layer theory*, Vol. 7. Springer.

Solomatov, V. and Moresi, L.N., 2000. "Scaling of time-dependent stagnant lid convection: Application to small-scale convection on earth and other terrestrial planets". *Journal of Geophysical Research: Solid Earth*, Vol. 105, No. B9, pp. 21795–21817.

Thomas, D.G., 1967a. "Enhancement of forced convection heat transfer coefficient using detached turbulence promoters". *Industrial Engineering Chemistry Process Design and Development*, Vol. 6, pp. 385–390.

Violato, D., Ianiro, A., Cardone, G. and Scarano, F., 2012. "Three-dimensional vortex dynamics and convective heat transfer in circular and chevron impinging jets". *International Journal of Heat and Fluid Flow*, Vol. 37, pp. 22–36.

Zhou, D.W., Lee, S., Ma, C. and Bergles, A., 2006. "Optimization of mesh screen for enhancing jet impingement heat transfer". *Heat and mass transfer*, Vol. 42, No. 6, pp. 501–510.

Zhou, D. and Lee, S.J., 2004. "Heat transfer enhancement of impinging jets using mesh screens". *International journal of heat and mass transfer*, Vol. 47, No. 10, pp. 2097–2108.

8. RESPONSIBILITY NOTICE

The following text, properly adapted to the number of authors, must be included in the last section of the paper:
The author(s) is (are) the only responsible for the printed material included in this paper.